# 竜巻飛来物（自動車）衝突による鉄筋コンクリート構造物の挙動

Performance of reinforced concrete structures due to vehicle impact during tornadoes

マドウラペルマ　マノジュ*, 丹羽一邦**
Manoj Madurapperuma,　Kazukuni Niwa

*Ph.D., 株式会社 テラバイト（〒113-0034 東京都文京区湯島 3 丁目 10 番 7 号　NOV ビル 3F）
**株式会社 テラバイト（〒113-0034 東京都文京区湯島 3 丁目 10 番 7 号　NOV ビル 3F）

*キーワード : concrete wall, numerical simulation, vehicle impact, tornadoes*

## 1. Introduction

Protection of critical structures against an accidental impact of a vehicle during tornadoes is becoming an important consideration particularly for critical facilities. In the present study, impact performance of reinforced concrete walls is evaluated using detailed finite element models of a vehicle and reinforced concrete walls. Thickness of the wall is varied to study damage mitigation measures. Different impact orientations are also considered to study severe impact scenarios. The study provides detailed information on the impact performance of reinforced concrete walls which will be useful for engineers and researchers.

## 2. Finite element modeling of vehicle impact on RC walls

To enable realistic simulation of impact between the vehicle and RC wall, LS-DYNA [1] is used and the finite element models incorporate inelastic material models with strain rate effects, material erosion to capture the failure process of damaged componenets in the vehicle and wall, and dynamic interaction between various parts of the vehicle and wall using appropriate contact algorithms. All simulations are carried out using an explicit solver where the time step is determined internally based on the smallest element size in the model and updated in each analysis step.

### 2.1 Vehicle model

A vehicle model created by the National Crash Analysis Center (NCAC) with George Washington University [2] was chosen for the present study. The model has been created using detailed vehicle geometry data and componenet level material tests, and has been validated for vehicle impact analysis.

The model used in the present study is the Ford Taurus (Fig. 1). The model consists of 26,793 nodes and 28,363 elements arranged in 133 parts with different material models. Nonlinear material models have been used in the most important parts of the vehicle such as bumper, rails, and frames. The total mass of the model is 2000 kg.

Fig.1 FE model used in the analysis

### 2.1 Wall model

Three types of walls are considered and has the same size of 5 m x 5 m. The thickness of walls is varied as 150 mm, 250 mm, and 450mm. The compressive strength of concrete is 22 MPa (the same value used in validation study) and the reinforcement raio is 0.8% by volume each way in all three walls. Details of rebar sizes are #4(12.7 mm) for 150 mm wall, #5(15.9 mm) for 250 mm wall, and #6(19.1 mm) for 450 mm wall. The yield strength of rebar is 345 MPa, tensile strength is 490 MPa and failure strain is 18%.

Solid elements and beam elements are used to model concrete and reinforcement, respectively. Perfect bond between concrete solid elements and reinforcement beam elements is considered. The constraints provided by beams and columns at the periphery are included in the model by constraining nodes on the surface of four-sides. Figure 2 shows wall size and rebar arrangement.

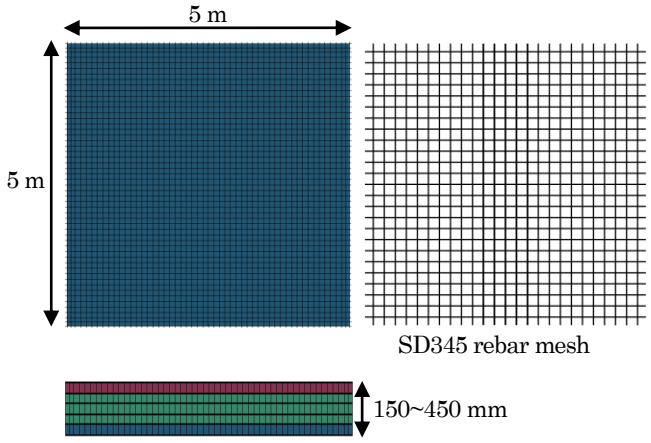


Fig.2 Wall configuration

The material model MAT_CONCRETE_DAMAGE_REL3 is chosen as the constitutive model for concrete [3,4]. This KCC material model has been extensively used for investigation of RC structural response to impact loads, and it is robust and has performed well in simulating experimentally oserved behavior. It is a three-invariant model that includes strain rate effect and damage. The selection of appropriate parameters for the KCC model is carried out by using experimental results of impact tests on RC walls as described in Section 3. The KCC model does not allow material erosion through removal of highly distorted elements from the model. Hence, complete removal of these distorted elements is considered using MAT_ADD_EROSION option which provides a way of automatically removal of elements from the calculation when the specified erosion criterion is satisfied. It is found from validation study and preliminary analysis of vehicle-wall impact that the appropriate values for maximum principal strain and shear strain are 0.1 and 0.1, respectively [4]. The material model MAT_PIECEWISE_LINEAR_PLASTICITY is used to model reinforcement.

Contact between the vehicle and wall is defined using a contact algorithm which has the capability to simulate eroding contacts, and self-contact among the vehicle components.

## 3. Impact test for validation of RC wall model

### 3.1 Description of the experiment

Full-scale impact tests have been carried out to investigate local damage to RC walls by the impact of aircraft engine [5]. The wall has the dimension of 7 m x 7 m x 1.6 m, unconfined compressive strength of concrete 22 MPa, reinforcement ratio of 0.8%. The wall was vertical and restrained at its four corners. The full-scale engine model was 0.76 m in diameter, 2.378 m in length and 1616 kg in mass, and it was allowed to impact at the center region of the wall at an impact velocity of 214 m/s.

### 3.2 Finite element model and comparison of results

As shown in Fig. 3, detailed quarter model is developed following the modeling procedure adopted for RC wall, as discussed in Section 2.1. Damage parameters in the KCC model is chosen to simulate experimentally observed damage behavior of the wall.

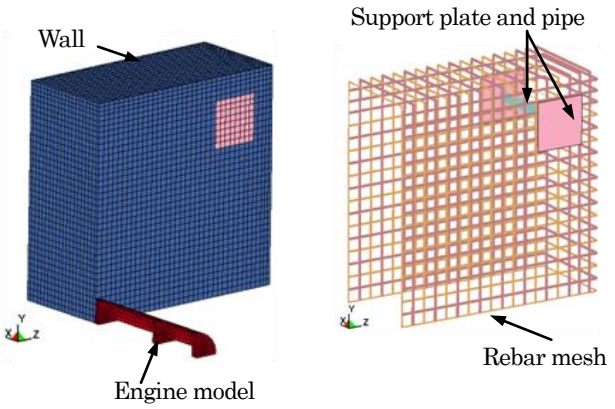


Fig. 3 Finite element model of engine impact on RC wall

Figure 4 compares displacement and total reaction force obtained in the simulation with the

experimental results. The displacement is measured at the center point back of the wall and the reaction forces are calculated at the restrained points. As shown in Fig. 4, analysis results show that displacement does not continuously increase due to failure of the front part of the engine which reduces impact load on the wall. The total reaction force does not continuously increase because of failure of the engine. Both peak displacement and peak reaction force are nearly the same as that of experiment. It has been reported that the depth of penetration was 210 mm and only cracks could be seen at the back of the wall in the experiment. The depth of penetration of the wall is 270 mm using the KCC model. It is seen that the calibrated model has the capability of simulating the damage behavior of the wall similar to damage behavior reported in the experiment.

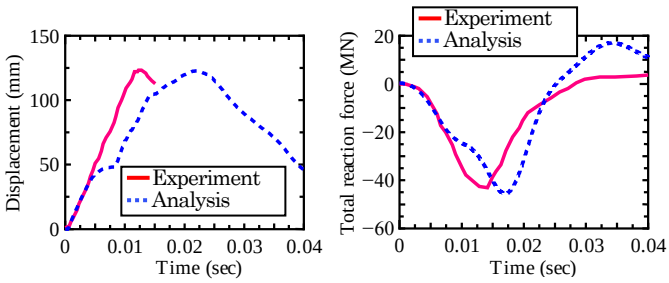


Fig. 4 Comparison of displacement and total reaction force

## 4. Vehicle-wall impact analysis and results

### 4.1 Analysis procedure

The impact velocity of the vehicle is 47 m/s which is widely used for impact assessment of buildings due to tornadoes. As shown in Fig. 5, two vehicle-wall impact configurations namely, front impact and side impact are considered in the analysis.

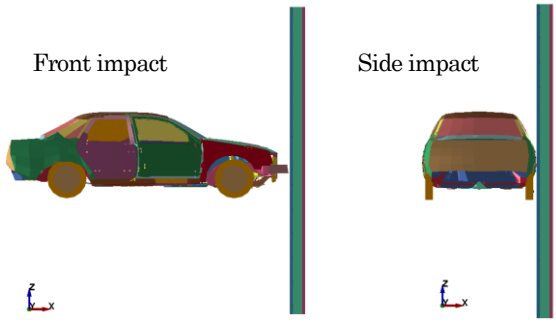


Fig. 5 Vehicle-wall impact configurations

### 4.2 Damage behavior

Figure 6 shows damage evolution of the 150 mm wall due to the front impact of the vehicle. The damage to the wall is severe where most of the concrete at the vicinity of the contact region in the front and back has removed.

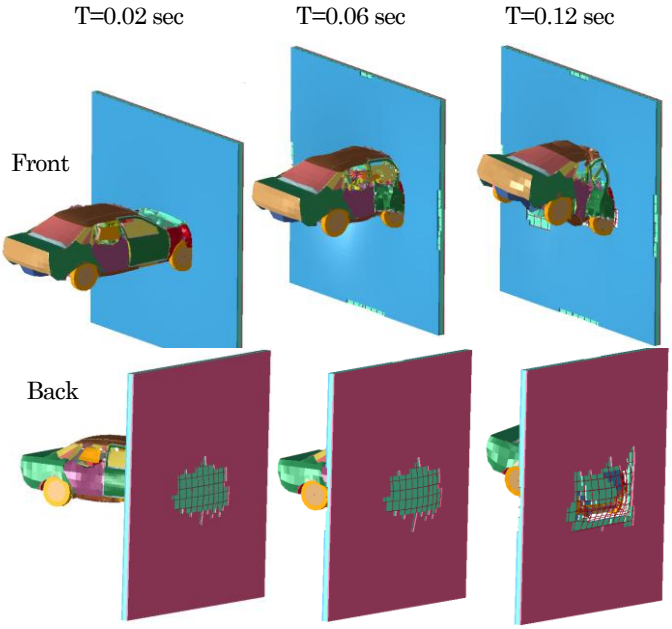


Fig. 6 Evolution of damage to the 150 mm wall due to the front impact of the vehicle

As shown in Figure 7, in front view of the wall, the left side suffers more damage compared to the right side. In the vehicle model the driving seat is located in left side, and therefore, stiff parts directly come into contact with the wall causing more damage.

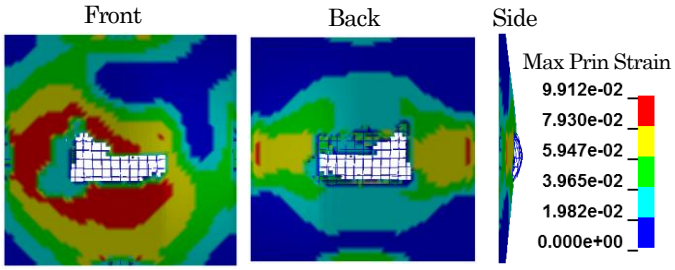


Fig. 7 Damage pattern of the 150 mm wall due to the front impact of the vehicle

Figure 8 shows damage evolution of the 150 mm wall due to the side impact of the vehicle. The damage to the wall is very severe where most of the concrete in the wall removed, rebar fails, and support edges of the wall suffer damage. As shown in Figure 9, in front view of the wall, the left side suffers more damage compare to the right side due to impact of engine and other heavy parts of the vehicle.

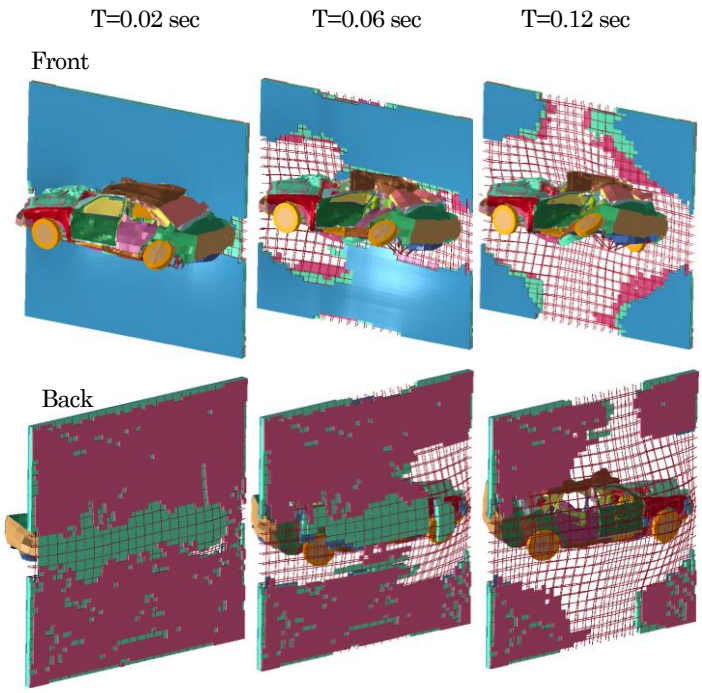


Fig. 8 Evolution of damage to the 150 mm wall due to the side impact of the vehicle

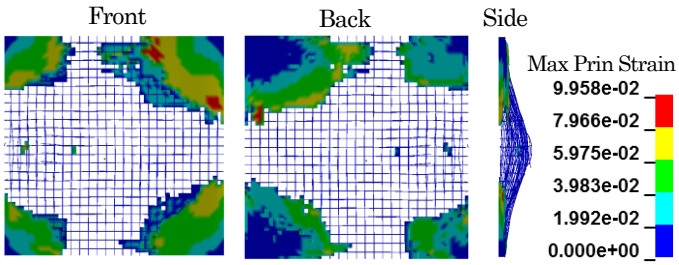


Fig. 9 Damage pattern of the 150 mm wall due to the side impact of the vehicle

Figure 10 shows damage evolution of the 250 mm wall due to the front impact of the vehicle. The damage to the wall is less compared to that of the 150 wall. The concrete in the back side has removed showing spalling damage to wall. Figure 11 shows damage is concentrated only to contact region, and the maximum principal strain is less than half of the specified concrete failure strain of 0.1.

Figure 12 shows damage evolution of the 250 mm wall due to the side impact of the vehicle. The damage to the wall is less compared to that of the 150 mm wall. The spalling damage to the wall is seen at an early stage of contact. As shown in Figure 13, in front view of the wall, the left side suffers more damage compared to the right side due to engine and most of other heavy parts of the vehicle are come into contact with the wall at the left side of the wall.

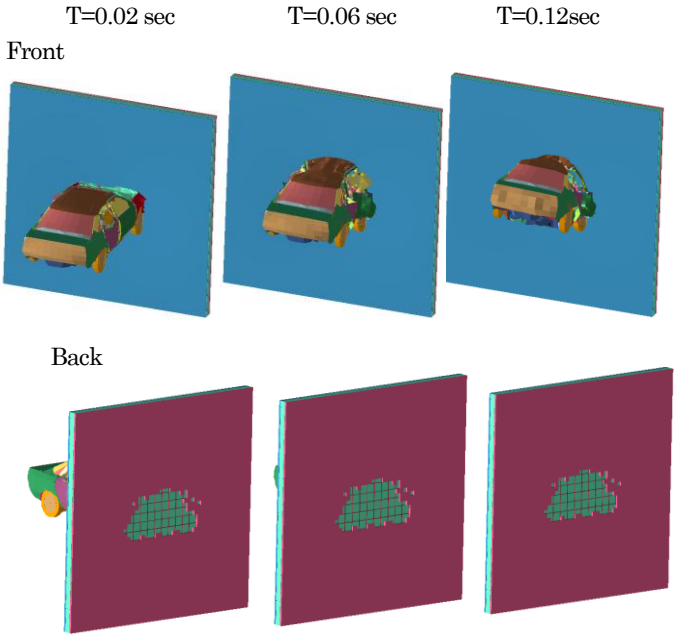


Fig. 10 Evolution of damage to the 250 mm wall due to the front impact of the vehicle

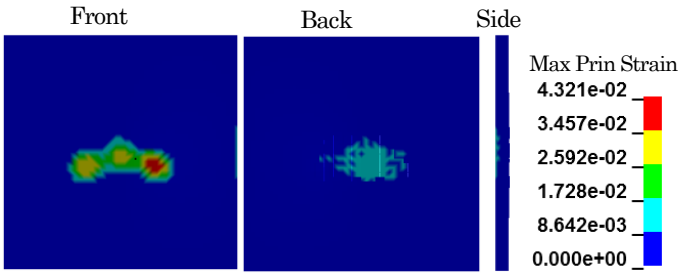


Fig. 11 Damage pattern of the 250 mm wall due to the front impact of the vehicle

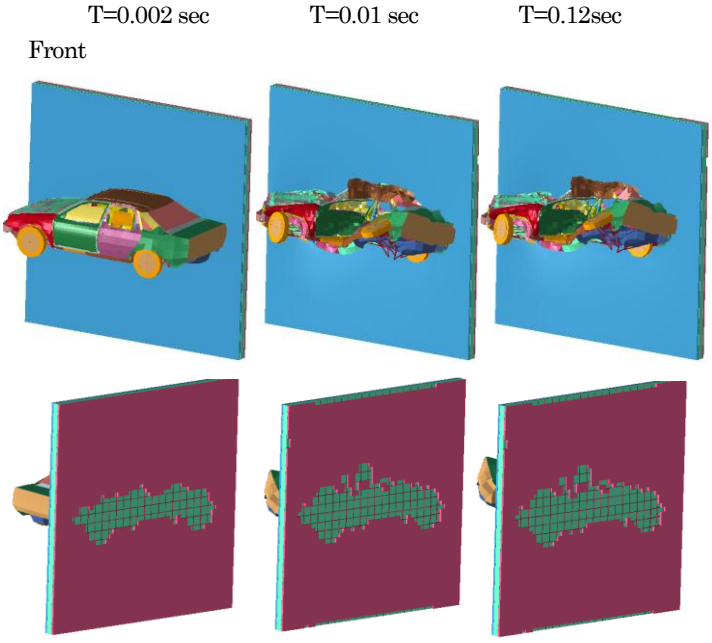


Fig. 12 Evolution of damage to the 250 mm wall due to the side impact of the vehicle

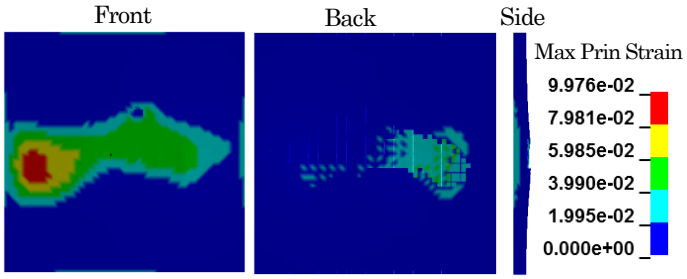


Fig. 13 Damage pattern of the 250 mm wall due to the front impact of the vehicle

Figure 14 shows damage evolution of the 450 mm wall due to the front impact of the vehicle. The damage to the wall is less compared to that of the 250 wall. The concrete in the back side has removed showing spalling damage to wall. Figure 15 shows damage is concentrated only to certain regions of the wall, and the maximum principal strain is less than one-third of the specified concrete failure strain of 0.1.

Figure 16 shows damage evolution of the 450 mm wall due to the side impact of the vehicle. The damage to the wall is less compared to that of the 250 mm wall. The spalling damage to the wall is seen at an early stage of contact. As shown in Figure 17, the maximum principal strain is 0.064 at severe damage regions of the wall, and it is less than the maximum principal stains of 150 mm and 250mm walls when the side impact of the vehicle.

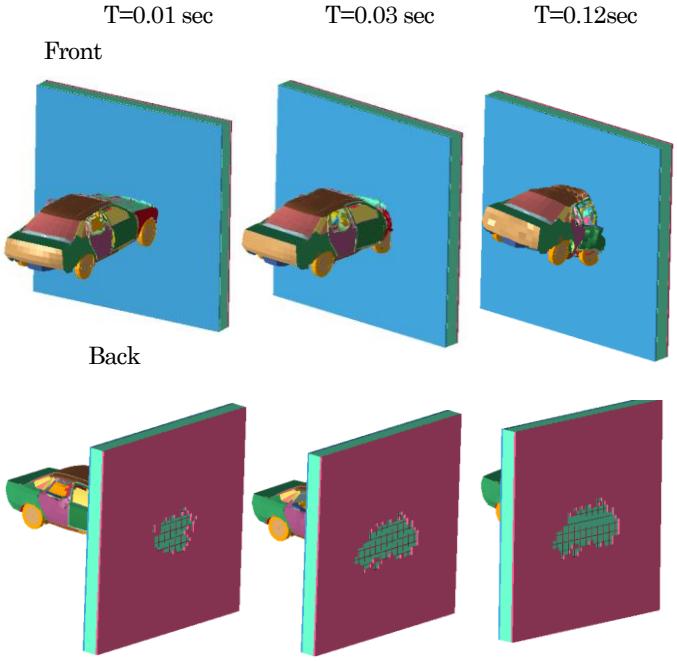


Fig. 14 Evolution of damage to the 450 mm wall due to the front impact of the vehicle

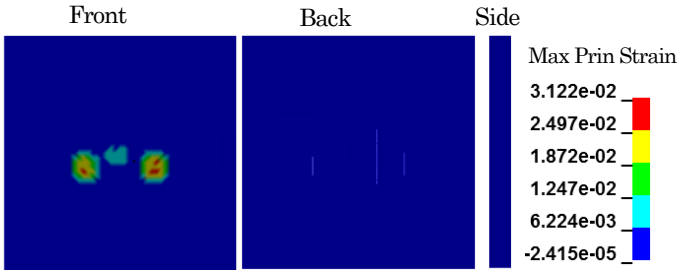


Fig. 15 Damage pattern of the 450 mm wall due to the front impact of the vehicle

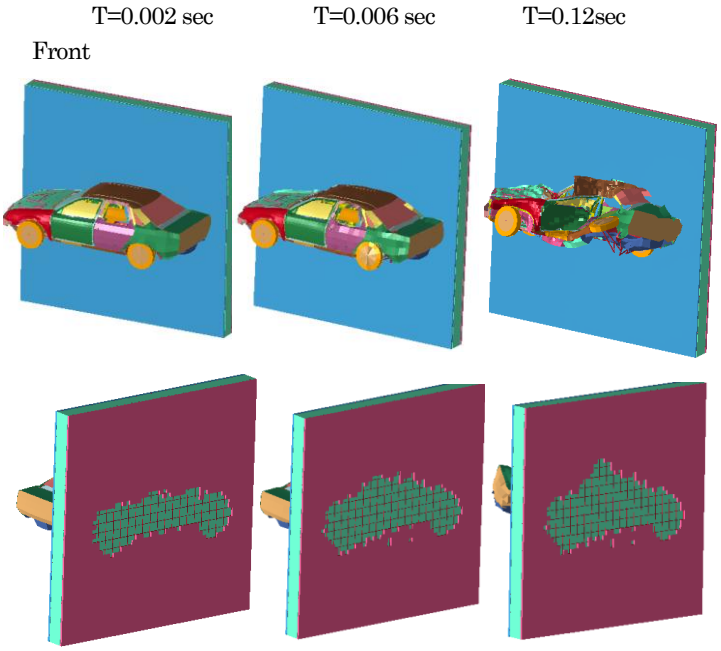


Fig. 16 Evolution of damage to the 450 mm wall due to the side impact of the vehicle

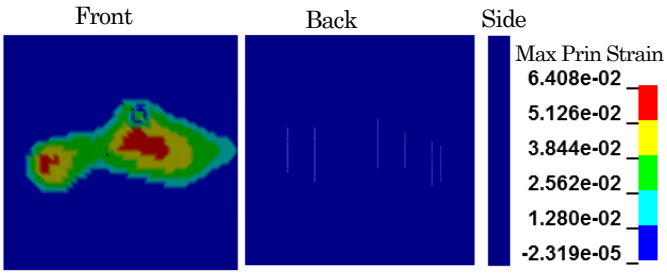


Fig. 17 Damage pattern of the 450 mm wall due to the front impact of the vehicle

## 5. Conclusions

For the vehicle considered, it is seen that side impact of the vehicle is more critical than front impact for the all three types of walls. Most of energy dissipators are designed for front impact of the vehicle and therefore, most of kinetic energy of the vehicle dissipated through plastic deformation of the vehicle when the vehicle front side impacts

on the walls. The side of the vehicle does not have such energy absorbers so that greater amount of kinetic energy can transfer to walls causing serere damage in the case of side impact. Further, the contact area is large in the case of side impact compared to front impact of the vehicle resulting large contact forces between vehicle and the wall which cause greater damage to the wall. It is seen that the increase of wall thickness considerably reduce damage to the wall. Furteher studies have to be carried out using other possible vehicle types which could become flying objects due to a tornado.

## References


1) LS-DYNA, Keyword User's Manual, Livermore Software Technology Corporation, CA (2013).
2) National Crash Analysis Center (NCAC), The George Washington University, USA < http://www.ncac.gwu.edu/>
3) Malvar, L.J., Crawford, J.E., Wesevich, J.W. and Simons, D., A Plasticity Concrete Material Model for DYNA3D, International Journal of Impact Engineering, Vol. 19, No. 9-10, pp. 847-873 (1997).
4) Madurapperuma, M., Niwa, K., Concrete Material Models in LS-DYNA for Impact Analysis of Reinforced Concrete Structures, Applied Mechanics and Materials, Vol. 566, pp. 173-178, (2014).
5) Sugano, T., Tsubota, H., Kasai, Y., Koshika, N., Ohnuma, H., von Riesemann, W.A., Bickel, D.C. and Parks, M.B., Local Damage to Reinforced Concrete Structures Caused by Impact of Aircraft Engine Missiles Part I: Test program, Method, and Results, Nuclear Engineering and Design, Vol. 140, (1993), p. 387-405.